Supporting information

Tensile Lattice Strain Accelerates Oxygen Surface Exchange and Diffusion in $La_{1-x}Sr_xCoO_{3-\delta}$ Thin Films

Markus Kubicek[†], Zhuhua Cai[‡], Wen Ma[‡], Bilge Yildiz[‡] Herbert Hutter[†], Jürgen Fleig[†]

[†] Institute of Chemical Technologies and Analytics, Vienna University of Technology, Getreidemarkt 9, A-1060 Vienna, Austria

[‡] Laboratory for Electrochemical Interfaces, Department of Nuclear Science and Engineering, Massachusetts Institute of Technology, 77 Massachusetts Avenue, Cambridge, Massachusetts 02139, United States

S1 Effect of chemical surface modification

Many perovskite-type oxides show a tendency for surface reconstruction and/or cation segregation at the surfaces. For LSC and similar materials such as $(La,Sr)(Co,Fe)O_{3-\delta}$ or $LaSrMnO_{3-\delta}$ a segregation of Sr to the surface is often observed.[1-7] Sr enriched surfaces are usually formed at elevated temperatures and frequently found to inhibit the oxygen reduction reaction.[2, 4-6] By chemical etching of the surface, Sr-rich material can be removed, exposing electrode material with bulk composition and higher catalytic activity to the gas phase.[1, 4] By etching for 5 seconds in 0.12 mol/l HCl, about 3 nm of the LSC thin films were removed from the surface. Tracer profiles after annealing as-prepared and etched LSC films on STO and LAO in $^{18}O_2$ at 400°C for 5 minutes are shown in Fig. S1. Etched thin films exhibited a higher surface exchange coefficients compared to as-prepared films. This fact corresponds to the larger tracer amount in etched films, clearly visible in Fig. S1. A small contribution of the increase of k* might also be caused by a slight roughening of the surface by the etching process. Differences in D* are found only for LSC/STO at 400°C and most probably reflect the large uncertainties for the very flat profiles, rather than true differences. However, the fact that after removing about 3 nm from the film surface the same effect of tensile over compressive strain on oxygen exchange is observed is further evidence that the films are fully strained over the whole 20 nm thickness. ^{18}O exchange of etched samples was performed together with non-etched samples, annealing parameters and k* and D* values are given in Tab. 1.

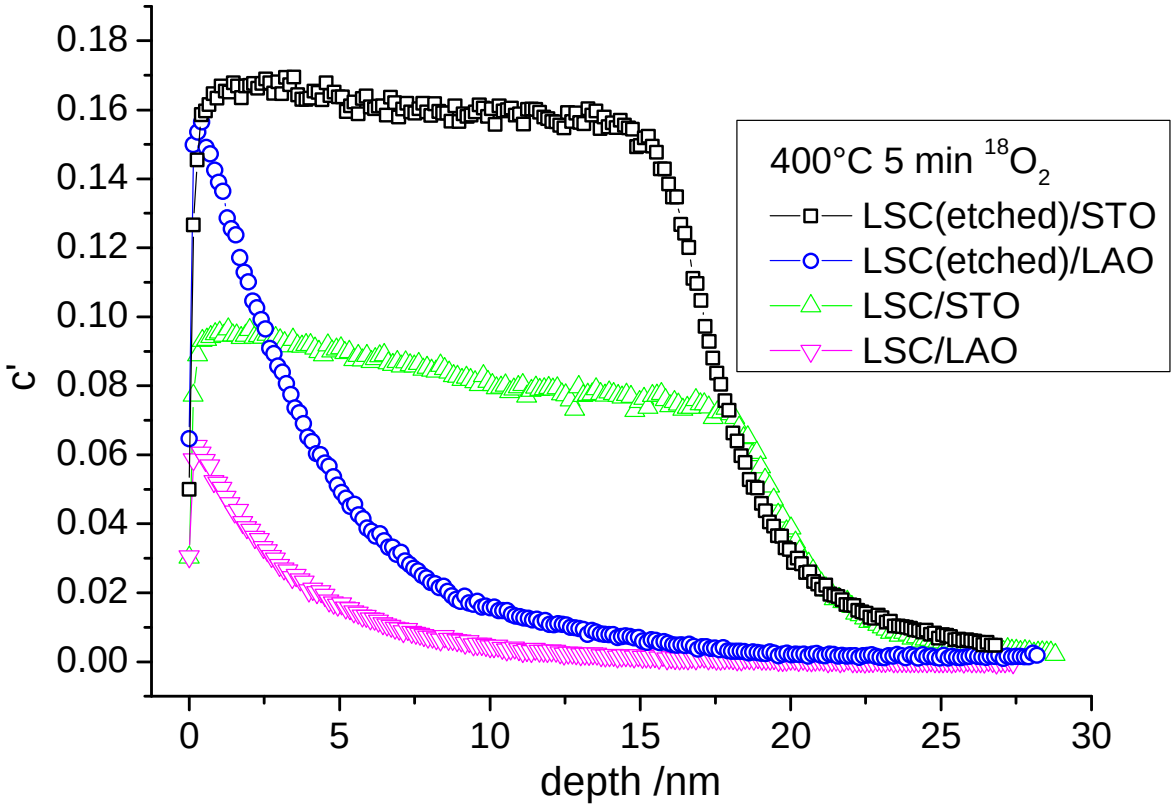

Figure S1: Tracer depth profiles comparing etched and as-prepared LSC82 thin films annealed together at 400°C for 5 minutes. Etched thin films exhibit a higher tracer surface exchange coefficient k.*

Table S1: Annealing parameters and fitted values of k and D* of etched LSC82 thin films. For D* values higher than 10^{-13} cm^2/s, no significant evaluation of D* is possible due to the almost flat tracer depth profiles.*

Sample	Time in $^{18}O_2$ / min	Temperature / °C	k* / 10^{-10} cm/s	D* / 10^{-15} cm²/s
LSC(etched)|STO	5	400	10.1	43
LSC(etched)|LAO	5	400	2.61	0.77
LSC|STO	5	400	5.83	19
LSC|LAO	5	400	0.967	0.80
LSC(etched)|STO	5	450	24.2	(>100)
LSC(etched)|LAO	5	450	9.34	3.7
LSC|STO	5	450	20.1	(>100)
LSC|LAO	5	450	8.45	3.9

S2 Films without predominant strain

In addition to strained LSC films, 20 nm LSC82 thin films grown on MgO without predominant strain state were investigated. The aim was to use LSC on MgO as a strain-neutral reference-sample to investigate whether the differences in oxygen surface exchange and diffusion observed in strained samples are caused by an activating effect of tensile strain or by inhibition from compressive strain, or if both effects are present. In Fig. S2, depth profiles of LSC thin films on MgO are compared to strained films on STO and LAO at 300°C and 400°C. The deduced parameters k* and D* for 300°C, 350°C and 400°C are given in Tab. S2.

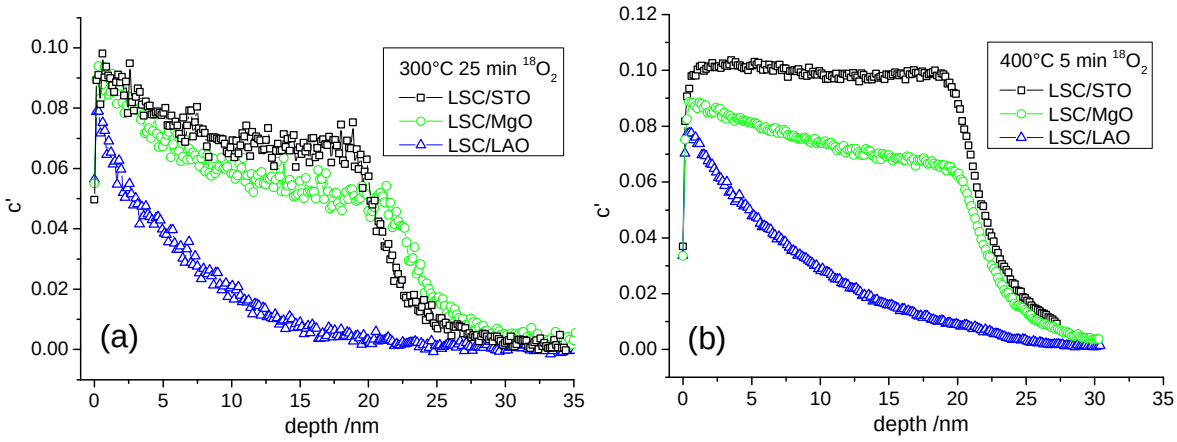

Figure S2: Tracer depth profiles comparing epitaxial and strained LSC82 on STO and LAO to non-epitaxial LSC82 on MgO without predominant strain at 300°C (a) and 400°C (b).

Table S2: Annealing parameters and fitted values of k and D* of strained epitaxial LSC82 thin films compared to polycrystalline films on MgO without predominant strain.*

Substrate	Time in $^{18}O_2$ / min	Temperature / °C	k* / 10^{-10} cm/s	D* / 10^{-15} cm²/s
STO	25	300	1.06	3.7
MgO	25	300	1.02	2.4
LAO	25	300	0.353	0.35
STO	5	350	2.24	5.8
MgO	5	350	1.63	5.3
LAO	5	350	0.557	0.72
STO	5	400	7.51	(80)
MgO	5	400	5.87	26
LAO	5	400	2.47	3.1

Thin films on MgO exhibit k* and D* values between those of the two strained films, but values are closer to the tensile strained LSC on STO, especially for low temperatures. This would suggest that both an activating effect for tensile strain and an even stronger deactivating effect of compressive strain are present. It has to be stated though, that for an unambiguous comparison an epitaxial (100) thin film on a blocking substrate without any strain throughout the whole temperature range would be needed. In case of the thin films on MgO it is probable that values of k* and D* are also affected by grain boundaries or different orientations of the surface. A final conclusion is therefore problematic. Recent experimental data and simulations[3, 8, 9] also suggest that both an activating and a deactivating effect can be observed depending on strain states. Those are attributed to changes of the near-surface oxygen vacancy concentration and electronic structure indicated by presence of Co^{2+} states measured by scanning tunneling microscopy and changes of the activation barrier in simulations on oxygen migration in the $LaCoO_3$-system.

S3 Different compositions of LSC

The strontium level in $La_{1-x}Sr_xCoO_{3-\delta}$ is known to strongly affect the electronic band structure as well as the oxygen non-stoichiometry.[10-13] Two different LSC-compositions, LSC82 and LSC64 were therefore investigated at different temperatures. Fig. S3 displays profiles for both compositions measured after annealing in $^{18}O_2$ at 375°C for 5 minutes and Tab. 3 contains the fitted values of k* and D*. Obviously, the higher Sr substitution level led to a higher surface exchange rate and diffusion coefficient in LSC64 thin films. Besides the higher absolute values, the same general dependence on the strain state was found with higher k* and D* for tensile strained LSC/STO. As a result of the higher diffusion coefficient, profiles of LSC64/STO are almost completely flat – therefore it can be concluded that D* is higher than for LSC82, but it is not possible to determine a value for D*. This effect of the higher Sr substitution level leading to faster oxygen exchange kinetics can be consistently found in results obtained on bulk LSC[14-18] and is often attributed to the higher concentration of oxygen vacancies in LSC64 and its different electronic structure. Also the higher D* value of LSC64 can, at least partly, be attributed to the higher oxygen vacancy concentration.

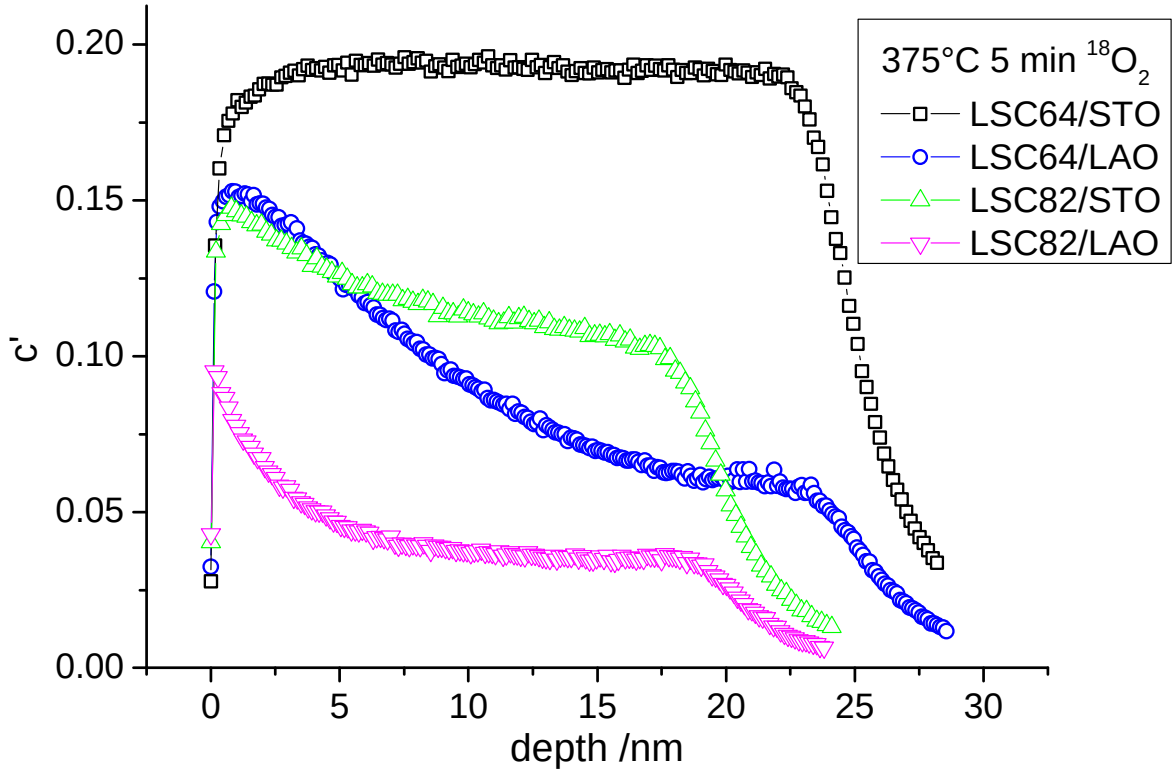

Figure S3: Tracer depth profiles comparing epitaxial and strained LSC films with the compositions $La_{0.8}Sr_{0.2}CoO_{3-\delta}$ (LSC82) and $La_{0.6}Sr_{0.4}CoO_{3-\delta}$ (LSC64). The higher Sr content in LSC64 leads to higher k and D* compared to LSC82, and the same tendency is found for the strain states (tensile>compressive) in both compositions.*

Table S3: Annealing parameters and fitted values of k and D* of strained LSC82 and LSC64 thin films at 325 and 375°C. For D* values higher than 10^{-13} cm^2/s, no significant evaluation of D* is possible due to the almost flat tracer depth profiles.*

Sample	Time in $^{18}O_2$ / min	Temperature / °C	k* / 10^{-10} cm/s	D* / 10^{-15} cm²/s
LSC64|STO	5	375	17.8	> 100
LSC64|LAO	5	375	8.21	8.1
LSC82|STO	5	375	8.63	16
LSC82|LAO	5	375	3.10	6.3
LSC64|STO	15	325	4.65	> 100
LSC64|LAO	15	325	1.24	0.95
LSC82|STO	15	325	1.31	2.4
LSC82|LAO	15	325	0.359	0.55

S4 Sample overview LSC82 temperature/time settings

Table S4: Values of k and D* of strained LSC82 and LSC64 thin films at 325 and 375°C corresponding depth profiles are partly shown in Fig. S3. For D* values higher than 10^{-13} cm^2/s, no significant evaluation of D* is possible due to the almost flat tracer depth profiles. Measurements at 280°C in brackets were performed to investigate the influence of chemical tracer incorporation.*

Substrate	Time in $^{18}O_2$ / min	Temperature / °C	k* / 10^{-10} cm/s	D* / 10^{-15} cm²/s
STO	4	475	30.8	(>100)
LAO	4	475	19.4	13
STO	5	450	20.1	(>100)
LAO	5	450	8.45	3.9
STO	5	425	16.9	(130)
LAO	5	425	7.03	5.6
STO	5	400	7.51	(80)
LAO	5	400	2.47	3.1
STO	5	400	5.83	19
LAO	5	400	0.967	0.80
STO	5	400	6.82	23
LAO	5	400	0.821	0.68
STO	5	375	8.63	16
STO	5	350	2.24	5.8
LAO	5	350	0.557	0.72
STO	15	325	1.31	2.4
STO	25	300	1.06	3.7
LAO	25	300	0.353	0.35
STO	30	300	1.11	3.3
LAO	30	300	0.36	0.42
STO	36	280	(0.51)	(1.5)
LAO	36	280	(0.26)	(0.52)
(STO*)	2	280	(3)	(10)
(STO*)	1	280	(4)	(13)

S5 Fitting curves for the investigated temperature range

Fitting curves are exemplarily shown for the whole temperature range of measurements on LSC82. For high temperatures and LSC82/STO very flat profiles are observed that even have the slight tendency to turn to “uphill” profiles which is a result of tracer re-exchange at the surface. Data of the lowest temperature, 280°C, were not used for evaluation as the effect of chemically driven tracer incorporation described in the Sec. “Limiations of the method and the temperature range” is observable and hampering the possibility to investigate the surface exchange and the diffusion coefficient.

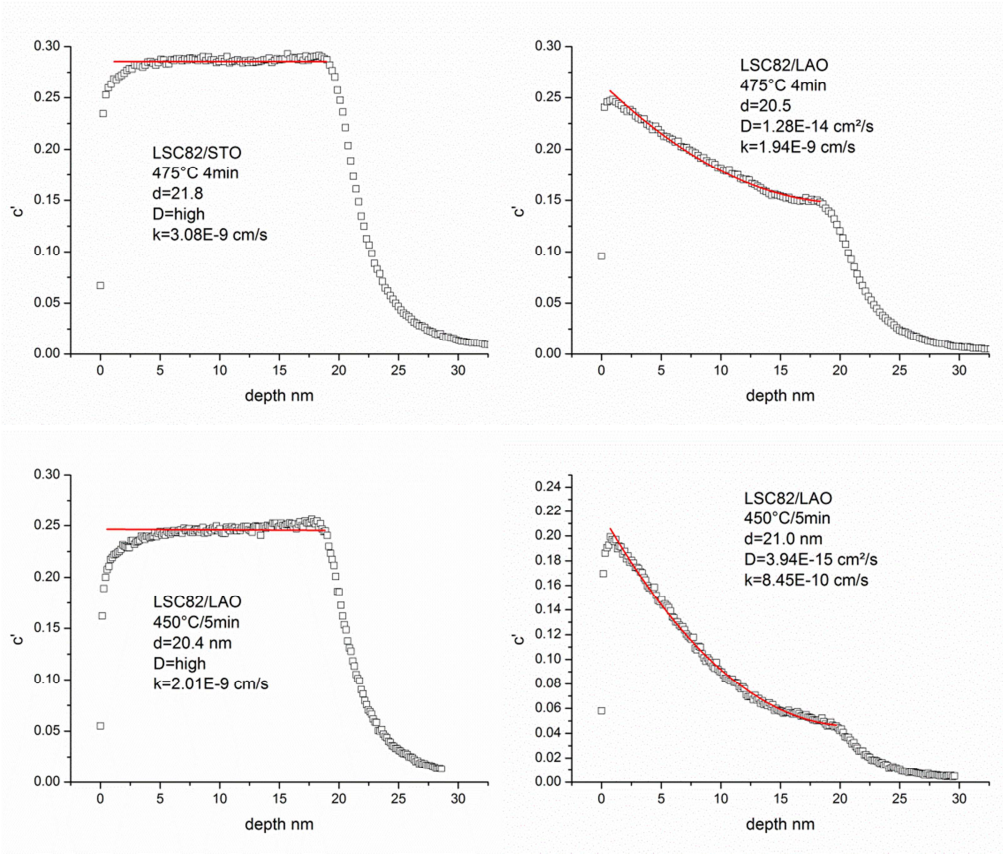

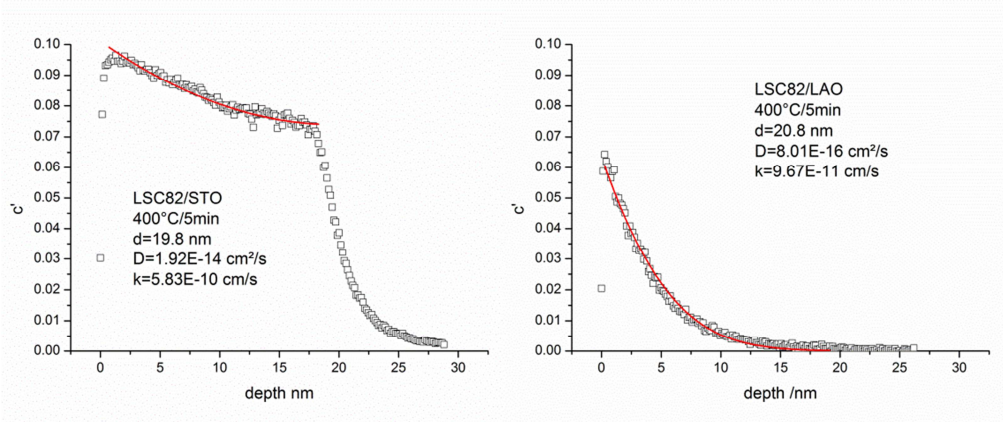
LSC82/STO
400°C/5min
d=19.8 nm
D=1.92E-14 cm²/s
k=5.83E-10 cm/s
c'
depth nm
LSC82/LAO
400°C/5min
d=20.8 nm
D=8.01E-16 cm²/s
k=9.67E-11 cm/s
c'
depth /nm

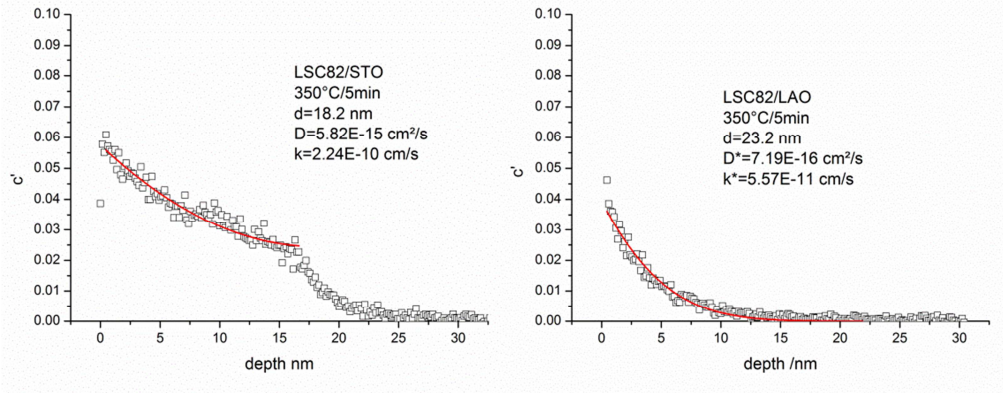
LSC82/STO
350°C/5min
d=18.2 nm
D=5.82E-15 cm²/s
k=2.24E-10 cm/s
c'
depth nm
LSC82/LAO
350°C/5min
d=23.2 nm
D*=7.19E-16 cm²/s
k*=5.57E-11 cm/s
c'
depth /nm

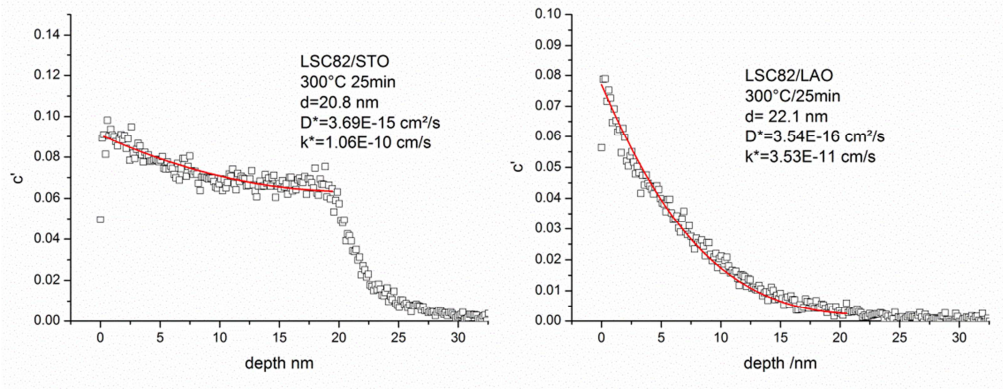
LSC82/STO
300°C 25min
d=20.8 nm
D*=3.69E-15 cm²/s
k*=1.06E-10 cm/s
c'
depth nm
LSC82/LAO
300°C/25min
d= 22.1 nm
D*=3.54E-16 cm²/s
k*=3.53E-11 cm/s
c'
depth /nm

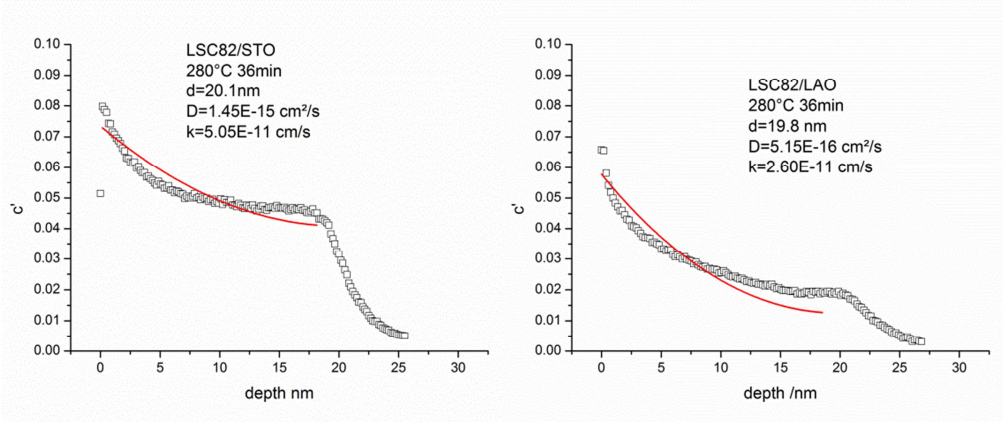

S6 CoO^- secondary ion signals

The CoO^- secondary ion signals were investigated in order to determine the position of the LSC|substrate interface. The sharpness of the interface was very similar for all investigated samples and confined to a zone of 2-3 nm. Consequently, an influence of cation diffusion on the determined values of k* and D* for oxygen could be neglected.

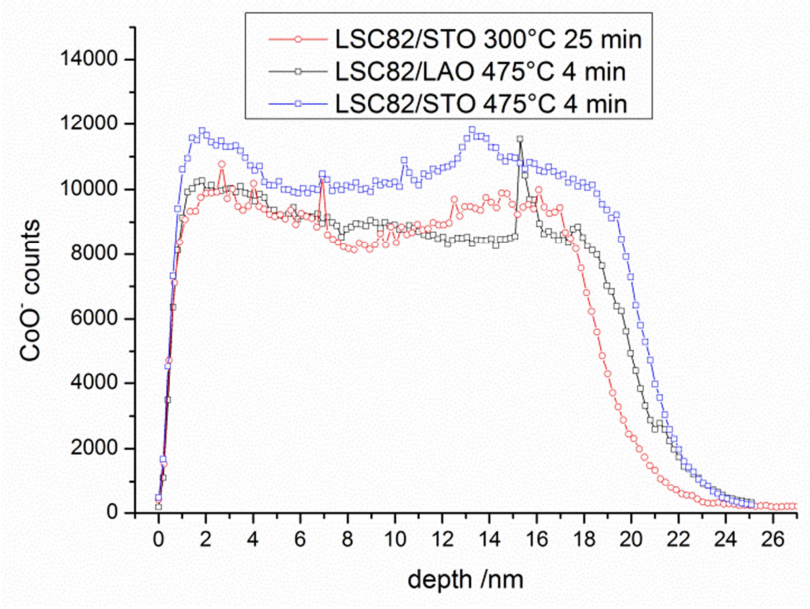

Figure S4: CoO^- secondary ion signals for measurements at different annealing temperatures. The slight changes of intensity with depth in LSC are due to fluctuations of primary ion intensity in SIMS measurements. Besides the known measurement related changes in the first 1-2 nm no general trend was found. At the interface the signal drops (90%-10%) within 2-3 nm and no trend of changes of the sharpness of the CoO^- drop between different samples was observed.

References

1. Jiang, S. P.; Love, J. G., Origin of the Initial Polarization Behavior of Sr-Doped $LaMnO_3$ for O_2 Reduction in Solid Oxide Fuel Cells. *Solid State Ionics* **2001**, 138, 183-190.
2. Hjalmarsson, P.; Sogaard, M.; Mogensen, M., Electrochemical Performance and Degradation of $(La_{0.6}Sr_{0.4})_{0.99}CoO_{3-delta}$ as Porous SOFC-Cathode. *Solid State Ionics* **2008**, 179, 1422-1426.
3. Cai, Z.; Kuru, Y.; Han, J. W.; Chen, Y.; Yildiz, B., Surface Electronic Structure Transitions at High Temperature on Perovskite Oxides: The Case of Strained $La_{0.8}Sr_{0.2}CoO_3$ Thin Films. *J. Am. Chem. Soc.* **2011**, 133, 17696-17704.
4. Kubicek, M.; Limbeck, A.; Frömling, T.; Hutter, H.; Fleig, J., Relationship between Cation Segregation and the Electrochemical Oxygen Reduction Kinetics of $La_{0.6}Sr_{0.4}CoO_{3-\delta}$ Thin Film Electrodes. *J. Electrochem. Soc.* **2011**, 158, B727-B734.
5. Bucher, E.; Sitte, W.; Klauser, F.; Bertel, E., Impact of Humid Atmospheres on Oxygen Exchange Properties, Surface-Near Elemental Composition, and Surface Morphology of $La_{0.6}Sr_{0.4}CoO_{3-delta}$. *Solid State Ionics* **2012**, 208, 43-51.
6. Oh, D.; Gostovic, D.; Wachsman, E. D., Mechanism of $La_{0.6}Sr_{0.4}Co_{0.2}Fe_{0.8}O_3$ Cathode Degradation. *J. Mater. Res.* **2012**, 27, 1992-1999.
7. Cai, Z. H.; Kubicek, M.; Fleig, J.; Yildiz, B., Chemical Heterogeneities on $La_{0.6}Sr_{0.4}CoO_{3-\delta}$ Thin Films-Correlations to Cathode Surface Activity and Stability. *Chem Mater* **2012**, 24, 1116-1127.
8. Jalili, H.; Han, J. W.; Kuru, Y.; Cai, Z. H.; Yildiz, B., New Insights into the Strain Coupling to Surface Chemistry, Electronic Structure, and Reactivity of $La_{0.7}Sr_{0.3}MnO_3$. *J Phys Chem Lett* **2011**, 2, 801-807.
9. Han, J. W.; Yildiz, B., Enhanced one Dimensional Mobility of Oxygen on Strained $LaCoO_3$(001) Surface. *J. Mater. Chem.* **2011**, 21, 18983-18990.
10. Señarís-Rodríguez, M. A.; Goodenough, J. B., Magnetic and Transport Properties of the System $La_{1-x}Sr_xCoO_{3-\delta}$ ($0 < x \leq 0.50$). *J. Solid State Chem.* **1995**, 118, 323-336.
11. Sitte, W.; Bucher, E.; Preis, W., Nonstoichiometry and Transport Properties of Strontium-Substituted Lanthanum Cobaltites. *Solid State Ionics* **2002**, 154–155, 517-522.
12. Efimov, V.; Efimova, E.; Karpinsky, A.; Kochubey, D. I.; Kriventsov, V.; Kuzmin, A.; Molodtsov, S.; Sikolenko, V.; Tiutiunnikov, S.; Troyanchuk, I. O.; Shmakov, A. N.; Vyalikh, A., XAFS and Neutron Diffraction Study of the $La_{1-x}Sr_xCoO_3$. *Phys Stat. Sol. C* **2007**, 4, 805-808.
13. Baskar, D.; Adler, S. B., High Temperature Magnetic Properties of Sr-Doped Lanthanum Cobalt Oxide $La_{1-x}Sr_xCoO_{3-\delta}$. *Chem Mater* **2008**, 20, 2624-2628.
14. Horita, T.; Yamaji, K.; Sakai, N.; Yokokawa, H.; Weber, A.; Ivers-Tiffée, E., Electrode Reaction of $La_{1-x}Sr_xCoO_{3-d}$ Cathodes on $La_{0.8}Sr_{0.2}Ga_{0.8}Mg_{0.2}O_{3-y}$ Electrolyte in Solid Oxide Fuel Cells. *J. Electrochem. Soc.* **2001**, 148, A456-A462.
15. Borovskikh, L.; Mazo, G.; Kemnitz, E., Reactivity of Oxygen of Complex Cobaltates $La_{1-x}Sr_xCoO_{3-\delta}$ and $LaSrCoO_4$. *Solid State Sciences* **2003**, 5, 409-417.
16. Adler, S. B., Mechanism and Kinetics of Oxygen Reduction on Porous $La_{1-x}Sr_xCoO_{3-\delta}$ Electrodes. *Solid State Ionics* **1998**, 111, 125-134.
17. De Souza, R. A.; Kilner, J. A., Oxygen Transport in $La_{1-x}Sr_xMn_{1-y}Co_yO_{3\pm\delta}$ Perovskites Part I. Oxygen tracer diffusion. *Solid State Ionics* **1998**, 106, 175-187.
18. De Souza, R. A.; Kilner, J. A., Oxygen Transport in $La_{1-x}Sr_xMn_{1-y}Co_yO_{3\pm\delta}$ Perovskites: Part II. Oxygen surface exchange. *Solid State Ionics* **1999**, 126, 153-161.